Boundary-Layer Meteorology (2006) 118: 477–501
DOI 10.1007/s10546-005-7772-y

VERTICAL STRUCTURE OF THE URBAN BOUNDARY LAYER OVER MARSEILLE UNDER SEA-BREEZE CONDITIONS

AUDE LEMONSU*, SOPHIE BASTIN[1], VALÉRY MASSON and PHILIPPE DROBINSKI[1]

Centre National de Recherches Météorologiques, Météo-France, 42 av. Coriolis, 31057 Toulouse Cedex, France; [1]*Institut Pierre Simon Laplace/Service d'Aéronomie, Université Pierre & Marie Curie, 4 place Jussieu, 75252 Paris Cedex 05, France*

(Received in final form 3 May 2005)

Abstract. During the UBL-ESCOMPTE program (June–July 2001), intensive observations were performed in Marseille (France). In particular, a Doppler lidar, located in the north of the city, provided radial velocity measurements on a 6-km radius area in the lowest 3 km of the troposphere. Thus, it is well adapted to document the vertical structure of the atmosphere above complex terrain, notably in Marseille, which is bordered by the Mediterranean sea and framed by numerous massifs. The present study focuses on the last day of the intensive observation period 2 (26 June 2001), which is characterized by a weak synoptic pressure gradient favouring the development of thermal circulations. Under such conditions, a complex stratification of the atmosphere is observed. Three-dimensional numerical simulations, with the Méso-NH atmospheric model including the town energy balance (TEB) urban parameterization, are conducted over south-eastern France. A complete evaluation of the model outputs was already performed at both regional and city scales. Here, the 250-m resolution outputs describing the vertical structure of the atmosphere above the Marseille area are compared to the Doppler lidar data, for which the spatial resolution is comparable. This joint analysis underscores the consistency between the atmospheric boundary layer (ABL) observed by the Doppler lidar and that modelled by Méso-NH. The observations and simulations reveal the presence of a shallow sea breeze (SSB) superimposed on a deep sea breeze (DSB) above Marseille during daytime. Because of the step-like shape of the Marseille coastline, the SSB is organized in two branches of different directions, which converge above the city centre. The analysis of the 250-m wind fields shows evidence of the role of the local topography on the local dynamics. Indeed, the topography tends to reinforce the SSB while it weakens the DSB. The ABL is directly affected by the different sea-breeze circulations, while the urban effects appear to be negligible.

Keywords: Atmospheric boundary layer, Doppler lidar, Numerical simulation, Sea breezes, Topography.

1. Introduction

Marseille is one of the biggest French cities with about 1 million inhabitants (Figure 1). Facing the Mediterranean sea, Marseille is frequently under the

* E-mail: aude.lemonsu@ec.gc.ca

influence of sea-breeze circulations during summertime. In fact, numerous big cities have been built in coastal areas and the urban canopy generally plays a key role on the local meteorology. Especially, the urban heat-island effect sometimes generates heat-island circulations above the agglomerations (e.g. Lemonsu and Masson, 2002). Besides, in a coastal environment, the sea/land temperature contrast induces sea-breeze circulations that may combine with the heat-island circulations. In addition to the proximity of the sea, Marseille is also located in a mountainous area. As a result, terrain heterogeneities (including topography) may induce local atmospheric circulations of various temporal and spatial scales, where urban, maritime and topographic effects interact. Since Marseille and its urbanized and industrialized suburbs are major sources of atmospheric pollutants, these local circulations may have a critical impact on the stagnation and the concentration of atmospheric pollutants in the region.

Despite the few existing studies on heat-island circulations and sea-breeze interactions in Tokyo (Yoshikado and Kondo, 1989; Yoshikado, 1990), Athens (Kambezidis et al., 1995), Kyoto and Osaka (Ohashi and Kida, 2002), their fine-scale structure (100-m scale) has never been investigated because the ability to observe natural three-dimensional atmospheric airflow patterns has progressed slowly. Indeed, the observation of such local circulations is a challenge. Up to now, experimental investigation of such atmospheric flows mainly relied on in-situ measurements, either ground-based (Pooler, 1963; Physick and Byron-Scott, 1977; Vukovich et al., 1979) or airborne (Finkele et al., 1995; Chiba et al., 1999), which do not provide simultaneous documentation of the temporal and the spatial variabilities of the flows.

In Marseille, the fine-scale complexity of the flow structure is even stronger and is due to the fact that multi-scale flows such as synoptic wind, land/sea breezes, urban breeze (also called heat-island circulation) and slope winds may interact. This problem justified the organization of a large-scale campaign in the Provence-Alpes-Côte d'Azur region called ESCOMPTE (ExperimentS to COnstrain Models of atmospheric Pollution and Transport of Emissions) (Cros et al., 2004) with its sub-program called UBL (Urban Boundary Layer)/ESCOMPTE dedicated to the study of the urban boundary layer in the Marseille area (Mestayer et al., 2005). In the framework of these field campaigns, remote sensors such as sodars, radars and Doppler and ozone lidars were deployed to improve the spatial and temporal coverage of the atmospheric flow over the city of Marseille. This instrumental set-up allowed us to document the complex layered structure under sea-breeze conditions over Marseille (Delbarre et al., 2005), to study the interaction between the sea breeze and the sloping terrain in the northern suburbs of Marseille (Bastin and Drobinski, 2005), and to analyse the

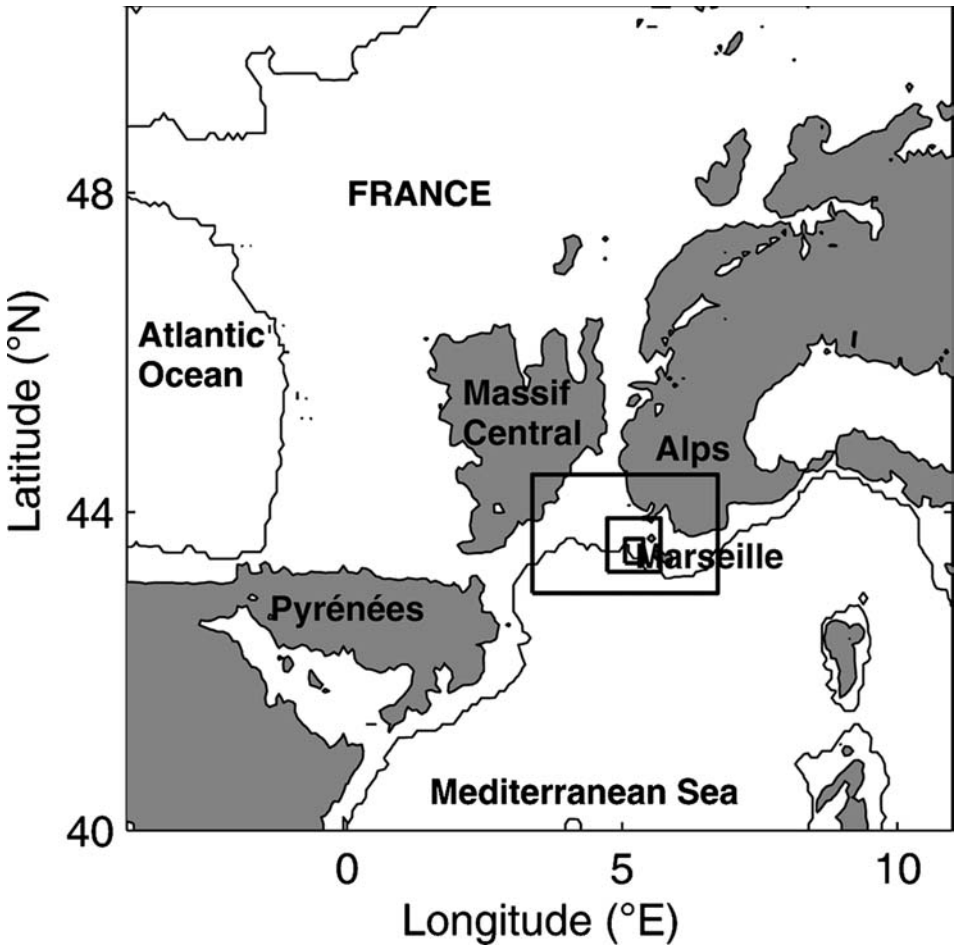

Figure 1. Map of France with the topography shaded in grey when higher than 500 m above sea level. The figure represents domain 1 (12-km horizontal resolution) of the Méso-NH simulation. The three rectangles display the three nested domains, hereafter called domain 2, 3 and 4 which have a 3-km, 1-km and 250-m horizontal resolution, respectively. Domain 4 is centred about the city of Marseille.

modification of the sea-breeze dynamics by the complex coastline shape of Marseille (Bastin et al., 2004).

However, the very fine scale heterogeneity of the flow over the city has never been analysed, and the relative contribution of the various sources of forcing of the flow (urban heating, topography, land/sea contrast,...) has never been investigated. In order to achieve this objective, we make use of wind measurements from a ground-based Doppler lidar, which was operated during ESCOMPTE and located at Vallon d'Ol in the northern suburbs of Marseille. Indeed, ground-based and airborne Doppler

lidars have already proved to be relevant tools to document land/sea breezes (Carroll, 1989; Banta et al., 1993; Banta, 1995; Darby et al., 2002; Bastin et al., 2004, 2005), and urban boundary layers (Calhoun et al., 2004; Davies et al., 2004). The Doppler lidar provides radial velocities at about 300-m spatial resolution in a volume covering a large domain both horizontally and vertically, with a temporal resolution and a wind measurement accuracy allowing the daily evolution of the flows to be finely described. In order to complement the Doppler lidar measurements, a numerical simulation with a 250-m horizontal resolution (i.e. similar to the Doppler lidar resolution) is performed with a specific urban parameterization (Masson, 2000; Lemonsu et al., 2004, 2005). This unique joint analysis of Doppler lidar measurements and very highly resolved model outputs allows a study of the dynamic and thermodynamic processes at the city scale. Specifically, our study analyses:

– the horizontal and vertical structure of the sea breeze at the city scale,
– the contribution of the topography to the local dynamics,
– the origin of the air masses that contribute to the complex horizontal and vertical structure of the urban boundary layer over Marseille.

This naturally requires a test of the ability of the numerical model to reproduce the vertical and horizontal fine-scale heterogeneity of the flow over Marseille, which has never been performed before.

After the introduction in Section 1, the experimental context and the numerical set-up are briefly presented in Sections 2 and 3, respectively. Section 4 presents a two-way comparison aiming at evaluating Méso-NH results with the Doppler lidar measurements. Sections 5 and 6 focus on the analysis of the processes involved in the vertical stratification of the atmosphere, and especially on the description of the various sea-breeze circulations that take place above Marseille. Section 7 concludes the study.

2. Experimental Context

2.1. Experimental domain

The field UBL-ESCOMPTE program (Mestayer et al., 2005) took place in the Marseille agglomeration from June to July 2001. Linked to the ESCOMPTE campaign (presented in detail in Cros et al., 2004), it specifically aims at documenting the thermo-radiative budget and the fluxes above the urban canopy layer, and also the four-dimensional structure of the UBL above the city. Marseille is one of the biggest French cities of about 1 million inhabitants and covers a 10 km by 15 km area. Its local geographic situation is especially complex (see Figure 2). It is located on the French

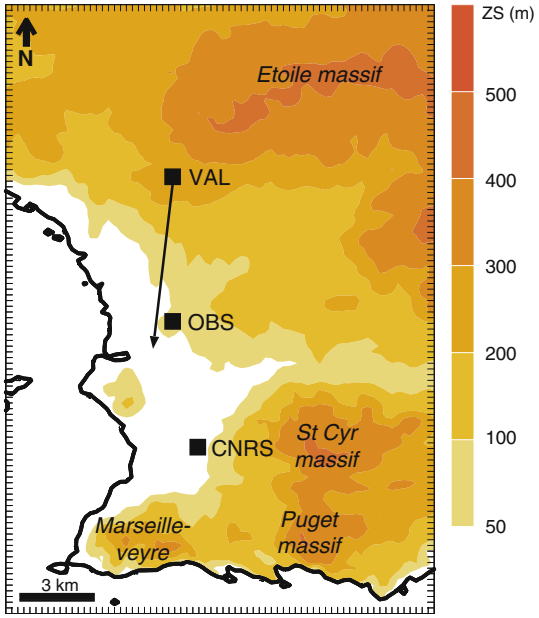

Figure 2. Marseille area. The squares label the location of the stations VAL, OBS and CNRS. The arrow represents the orientation of the line of sight used with the transportable wind lidar (TWL).

Mediterranean coast (both south and west of the city are edged by the sea), and is skirted by the Etoile massif (600 m) to the north, Saint Cyr (600 m) and Puget (550 m) massifs to the east, and the Marseilleveyre massif (450 m) to the south-west. In summertime, sea breezes frequently occur during the afternoon in all the coastal areas of the Provence-Alpes Côte d'Azur region. In the first hundreds of metres, the sea breeze flows perpendicularly to the coastline (Bastin et al., 2004; Bastin and Drobinski, 2005) whereas at higher levels (up to about 1500 m above ground level (a.g.l.), see Bastin et al., 2005) and in the rest of the region, where the coast is rather oriented from east to west, the sea breeze flows from the south-west. Situations of Mistral (strong north-westerly wind channelled within the Rhône valley, see Drobinski et al., 2005a; Guénard et al., 2005) and south-east winds also affect the region and can reach Marseille.

A large network covered the Provence-Alpes Côte d'Azur region for the ESCOMPTE campaign, while a specific network was deployed in Marseille area in the framework of the UBL project. This latter study, presented by Mestayer et al. (2005), is composed of meteorological stations, flux stations (Grimmond et al., 2004), wind profilers (Delbarre et al., 2005) and a ground-based Doppler lidar, hereafter called the transportable wind lidar (TWL) (Bastin et al., 2005). Intensive observation periods (IOP) were conducted, in cases of specific meteorological situations

favouring atmospheric pollution episodes. Some complementary experimental systems were operated during these IOPs.

2.2. Transportable wind lidar description

The present study mainly uses the measurements of the TWL, which was operated during the whole experiment. The TWL, operating at 10.6 μm in the infrared spectral region, was located at Vallon d'Ol (labelled VAL) (43.36° N, 5.40° E) in the northern districts of Marseille on the southern face of the Etoile massif ($z = 285$ m above sea level (a.s.l.)) (Figure 2). At 10.6-μm wavelength, the lidar signals are extremely sensitive to microscopic aerosols that are excellent tracers of the dynamics in the troposphere, therefore making the TWL a relevant tool for the study of the atmospheric boundary-layer (ABL) dynamics in complex terrain, such as urban areas (Drobinski et al., 1998), mountainous regions (Drobinski et al., 2001a, 2003) or in coastal areas (Bastin et al., 2005). The TWL provides radial wind velocity measurements along the line-of-sight (LOS) of the transmitted laser beam. The TWL radial range resolution and wind velocity accuracy are about 300 m and 0.3 m s^{-1}, respectively. The TWL scanning strategy consisted of vertical-slices (constant azimuth while varying in elevation, also called range-height indicator (RHI)) at azimuth angles separated by 30°. The TWL thus spatially documented the vertical structure of the atmosphere, by providing the radial velocities on a 6-km radius area and in the first 3 km of the troposphere. In the present study, we will analyse in detail the RHI performed at an azimuth angle of 190° from the north (from VAL towards the city core, see Figure 2). For this azimuth angle, a positive (negative) radial velocity indicates that the flow has a northerly (southerly) component for flow away from (toward) the TWL. A wind direction quasi normal to the LOS induces very weak radial velocities.

An ozone lidar was operated at VAL during the campaign, as well as a UHF radar at the Marseille Observatory (OBS, 43.31° N, 5.40° E, $z = 97$ m a.s.l.), located downtown, and a UHF sodar at the CNRS institute (CNRS, 43.26° N, 5.41° E, $z = 54$ m a.s.l.), south of the city. Surface stations were also installed there. VAL, OBS and CNRS are all labelled in Figure 2. OBS is almost on the LOS of the TWL, while CNRS is 10.5 km south-east of VAL.

2.3. Meteorological situation

Figure 3 presents the synoptic charts on 26 June 2001 at 0000 (panel (a)) and 1200 Universal Time Coordinate (UTC) (panel (b)). On 26 June 2001, a ridge at 500 hPa is over France generating a westerly synoptic flow at that

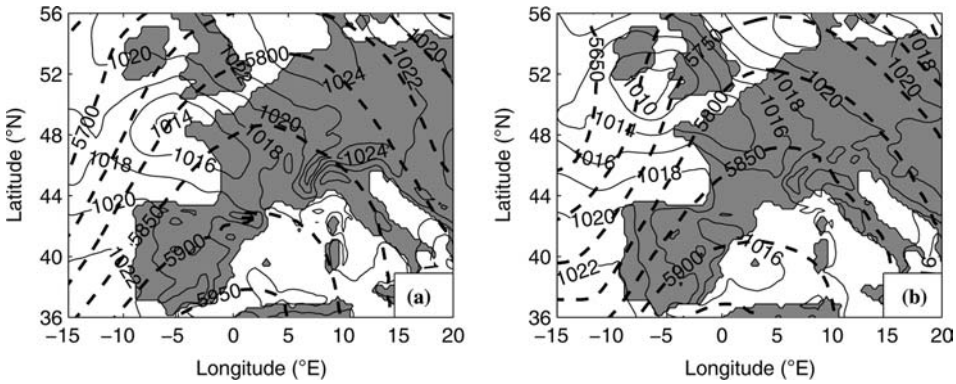

Figure 3. Synoptic charts from the European Center for Medium-range Weather Forecasts (ECMWF) analyses, showing the geopotential height at 500 hPa (thick dashed lines with an isocontour interval of 50 m) and the surface pressure field (solid line with an isocontour interval of 2 hPa) on 26 June 2001 at 0000 (panel a) and 1200 UTC (panel b).

level. A surface pressure anticyclone is located over northern Europe and its intensity slightly decreases between 0000 and 1200 UTC. In the same time, a surface pressure low is deepening from 1014 hPa at 0000 UTC to 1010 hPa at 1200 UTC. It is located over western France at 0000 UTC and moves northwards. The Açores surface pressure high stagnates over western Africa. Consequently, the horizontal pressure gradient over southern France is weak. Nevertheless, a weak surface pressure low forms over Baleares between 0000 and 1200 UTC, inducing a weak southerly flow over the target area in the afternoon. Conditions are propitious for the development of a sea-breeze circulation. The weather is hot (about 35 °C inland) and the atmosphere is very sultry generating local thunderstorms at the end of the afternoon. Based on the above observations, a pollution episode is predicted to occur during IOP 2B (24–26 June 2001).

Figure 4 presents the time evolution of the surface wind speed and wind direction, and surface air temperature at Marseille (43.3° N, 5.4° E) and 30 km inland at Aix en Provence (43.5° N, 5.4° E) on 26 June 2001. At night, the temperature difference between Aix en Provence and Marseille, located on the coast, is negative (about −5 °C), showing evidence of a weak land breeze (about 1 m s^{-1}) flowing from the north in Aix and from the east in Marseille, i.e. perpendicular to the coastline. At night, the wind speed is weak (less than 2 m s^{-1}) so that the wind direction is hardly reliable. At 0800 UTC, the temperature difference shifts from negative to positive values (about +5 °C at 1200 UTC) indicating the onset of the sea breeze, associated with a 180° rotation of the wind direction and an increase of the wind speed (to about 6 m s^{-1}). Note that the local solar time, which is a relevant time coordinate for breeze studies, corresponds to UTC +20 min. Because of this small difference, we use the UTC time unit.

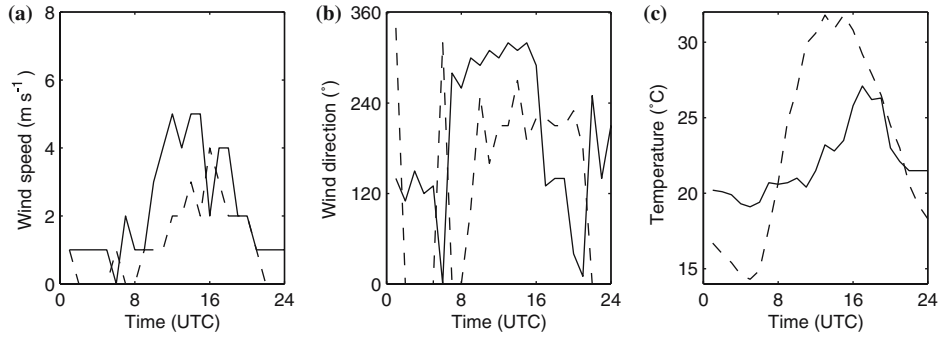

Figure 4. Time evolution of wind speed (a), wind direction (b) and temperature (c) on 26 June 2001 from surface meteorological stations data collected at Marseille (solid line) and Aix en Provence (dashed line). The time resolution is 1 h and the wind speed accuracy is $\pm 0.5\,\mathrm{m\,s^{-1}}$. The absence of data in panel (b) corresponds to zero wind speed (wind direction has no meaning).

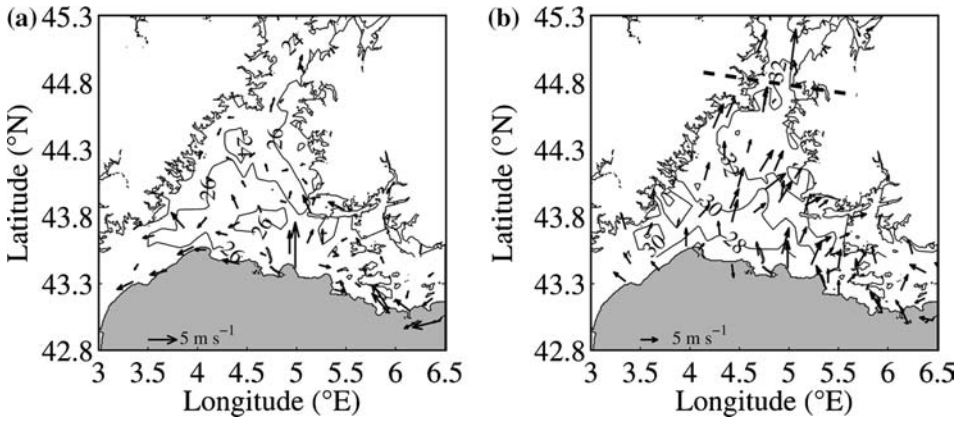

Figure 5. Wind field from meteorological surface stations on 26 June 2001 at 0800 UTC (a) and 1600 UTC (b). Arrows indicate the wind direction and they are scaled to fit within the wind intensity. The isotherms are solid lines with an increment step of 2 °C. The grey area corresponds to the Mediterranean sea and the thick dashed line in (b) marks the sea-breeze front position.

Figure 5 displays the surface wind and temperature fields on 26 June 2001 at 0800 and 1600 UTC. At 0800 UTC, the temperature field reveals the absence of a sea breeze, and the prevailing southerly wind is weak (less than 2–3 $\mathrm{m\,s^{-1}}$). At 1600 UTC, the air temperature increases from 28 °C near the coast to 32 °C at 44.8° N (near Orange), where the sea-breeze front stabilizes. The weakening temperature gradient and the delay in the sea-breeze establishment (compared for instance to the 25 June 2001 case described by Bastin et al., 2004, 2005) are consistent with Estoque (1962)

who shows numerically that an onshore large-scale wind advects cold air over land and thus inhibits the temperature rise.

3. Numerical Set-up

The three-dimensional simulations are performed with the Méso-NH non-hydrostatic atmospheric model (Lafore et al., 1998). The details of the set-up are presented in Lemonsu et al. (2005). Four nested models, with successive horizontal grid resolutions of 12 km, 3 km, 1 km and 250 m, are used (Figure 1). The vertical grid has 52 levels with 28 levels below 1500 m. For the highest resolution, the turbulence scheme uses a three-dimensional calculation, based on the large-eddy simulation parameterization of Deardorff (1974). The initial conditions of the four models and the model 1 boundary conditions are given by the European Center for Medium-range Weather Forecasts (ECMWF) analyses. The sea surface temperature (SST), given by the ECMWF analyses for models 1 and 2, is replaced for models 3 and 4 by the National Atmospheric and Oceanic Administration (NOAA) advanced very high resolution radiometer (AVHRR) satellite data, which have a finer resolution (Dousset and Kermadi, 2003).

Méso-NH is run with the interactive soil biosphere atmosphere (ISBA) (Noilhan and Planton, 1989) and the town energy balance (TEB) (Masson, 2000) schemes, to parameterize the surface exchanges for the natural soils and the vegetation, and for the built-up areas, respectively. The Marseille land cover map is provided by the regional centre of geographic information (CRIGE) at 30-m resolution, based on the CORINE land cover classification (CEC, 1993). Note that an extensive off-line evaluation against energy fluxes of the ISBA-TEB was conducted in the city core (Lemonsu et al., 2004). The topographic fields are defined at 1-km horizontal resolution for models 1 and 2, and at 250-m horizontal resolution for models 3 and 4.

The IOP 2B (24–26 June 2001) is simulated with an initial spin-up of 12 h. A complete validation at both regional and city scales was conducted for the whole period against most of the available observations (Lemonsu et al., 2005). Méso-NH correctly reproduces the evolution of the regional meteorological conditions and of the vertical structure of the ABL. The fine structure of the daytime thermodynamical fields above Marseille, which evolves according to the situations and the predominant flows, is also well modelled. Specific attention was focused on the 22 and 26 June 2001 to underscore the variability of the vertical structure of the UBL over Marseille.

4. Comparison of the TWL and the Model

The fine-scale simulated flow from model 4 at 250-m horizontal resolution can be compared to the observations made by the TWL at a similar resolution (about 300 m). To do so, similar simulated radial velocity fields are computed from model 4 flow using the relation between the radial velocity and the three components of the wind:

$$v_r = U \cos\phi \sin\psi + V \cos\phi \cos\psi - w \sin\phi, \quad (1)$$

where U is the zonal wind component, V the meridional wind component, w the vertical wind speed, ϕ the elevation angle and ψ the azimuth angle. Figure 6 shows the comparison between the radial velocities from the TWL (left row) and from model 4 (right row) for three RHI scans across the northern district of Marseille, at 190° from the north, performed by the TWL at 1030, 1400 and 1700 UTC.

At 1030 UTC, the TWL data indicate the superimposition of three layers (labelled *B*, *C*, and *D* in Figure 6a), where the radial velocities are globally negative. Layer *B* reaches 1100 m a.s.l. with radial velocities of about $-4\,\mathrm{m\,s^{-1}}$. However, beyond 4.5 km away from the TWL, the velocities are weaker (less than $2\,\mathrm{m\,s^{-1}}$). Thus, the wind blows towards the TWL in the northern districts, while above the city core it is either very weak or quasi perpendicular to the LOS. Between 1100 and 1700 m a.s.l., at VAL and between 1100 and 1400 m a.s.l., between 5 and 7 km south of VAL (corresponding to layer *C*), the radial velocities are close to zero everywhere. Above layer *C*, a layer of negative radial velocities is observed (layer *D*), indicating flow towards the TWL. The model also predicts four distinct layers (labelled *A*, *B*, *C*, and *D* in Figure 6b). Layer *A* reaches 350 m a.s.l., i.e. ≈200 m above the ground level (a.g.l.) and the radial velocities are positive in the morning. Layer *A* is not visible in the TWL measurements since, on 26 June 2001, the TWL data were not reliable between 300 and 600 m a.s.l. (i.e. 300 m a.g.l. at VAL). Above layer *A*, the model simulates two layers of negative velocities: (1) layer *B* is located between 300 and 800 m a.s.l. above the city core and between 400 and 900 m a.s.l. above VAL; (2) layer *D* is in altitude, beyond 1200 m a.s.l. above the city core and 1500 m a.s.l. above VAL. Between layers *B* and *D* (layer *C*), the velocities are very weak as in the observations, but rather positive. This may be due to a small difference between the measured and simulated wind directions with respect to the LOS azimuth. Layer *C* is 500 m deep above VAL and 300 m deep to the south in agreement with the TWL, but the altitude of the simulated layer *C* is about 200 m too low in comparison to the measurements.

At 1400 UTC, the vertical structure is very similar to that documented in the morning (Figure 6c), although the tops of layers *B* and *C* are higher: 1300 and 1850 m a.s.l. at 1400 UTC versus 1100 and 1700 m a.s.l. in the

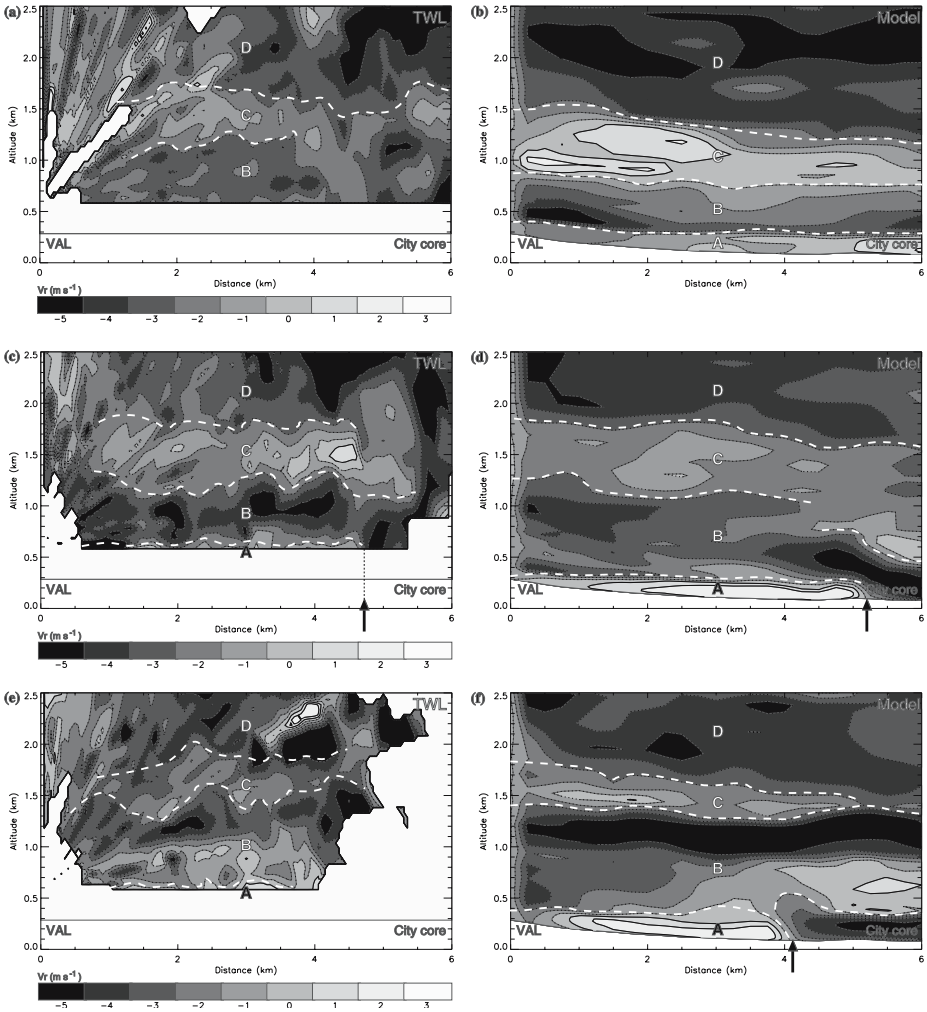

Figure 6. Vertical cross-sections of observed (left row) and modelled (right row) radial velocities along the LOS (labelled in Figure 3), at 1100 UTC (top), 1400 UTC (middle) and 1700 UTC (bottom). The solid and the dashed isolines distinguish the positive and the negative radial velocities, respectively. The model outputs correspond to model 4, which has a horizontal resolution similar to that of the TWL measurements.

morning, respectively. The flow pattern evolves near the surface: (1) the TWL measures positive radial velocities up to 600–700 m a.s.l. to a distance of 4.7 km away from the TWL. This layer corresponds to layer *A*, simulated by the model at 1100 UTC; (2) beyond 4.7 km south of VAL, the TWL records negative velocities near the surface. This change of sign of the radial velocity illustrates the convergence between a flow with a northerly component and a flow with a southerly component above the city

core. This process is also underscored by the ground-based station at OBS (Delbarre et al., 2005) with a southerly flow after 1300 UTC. In the simulation, a region of negative velocities also appears but it is beyond 5.3 km from VAL (Figure 6d), which is about 1 km to the south in comparison to the observations. However, the location of the front at the surface cannot be accurately estimated with the TWL, since the data are not reliable below 300 m a.g.l. Layers *B*, *C* and *D* are very similar to those identified from the TWL data, in terms of location and associated radial velocities. Notably, the layer of weak radial velocities, between 1200 and 1900 m, is better located in the model at 1400 UTC than at 1030 UTC. However, note that the altitude of the simulated layer *A* is underestimated with respect to the TWL measurements: it reaches 400 m in the simulation versus 600–700 m a.s.l. in the observations.

The TWL measurements display more variability at 1700 UTC than at 1030 and 1400 UTC, and show that the layering still evolves in the afternoon (Figure 6e). A very low layer of positive radial velocities persists near the surface up to 4.0 km south of the TWL (layer *A*). More to the south, no measurements are available. Between 600 and 1000 m a.s.l., layer *B* is characterized by very weak negative velocities. A thin layer above, between 1000 and 1500 m a.s.l., is defined by flow towards the TWL (with stronger negative radial velocities). This layer was not observed previously. The velocities are again very weak between 1500 and 1900 m a.s.l. in layer *C*, and more negative in layer *D*. The structure also evolves in the simulation (Figure 6f). The region of negative radial velocities near the surface, which was already underscored at 1400 UTC, still progresses to the north and is now located 4.2 km south of VAL. Although the southerly flow is actually beyond OBS, its penetration is slightly overestimated in the model, because it is not observed with the TWL, which has a maximum horizontal range of 4 km in the lower levels. Both weak velocity layers *B* and *C* between 450 and 1000 m a.s.l., and between 1300 and 1600 m a.s.l., are correctly located, as well as the layer of strong radial velocities between layers *B* and *C*.

5. Regional-Scale Description of the Flows

The complex layering of the atmosphere above Marseille, underscored by the TWL on 26 June 2001, is also confirmed by the other observational systems, especially the UV lidar at VAL and the UHF radar at OBS (Delbarre et al., 2005). In order to understand and to interpret these structures, modelling is an efficient tool to analyse the dynamical processes involved. Here we present a joint study of the back-trajectories, and the wind fields produced by the models at the regional scale.

5.1. Synoptic flows

At the regional scale, the back-trajectories indicate the origin of the air masses that are identified as the successive layers discussed in Section 4. The back-trajectories are calculated from the hourly model 2 outputs (3-km horizontal resolution) for the air parcels that arrive at VAL, at OBS, and at CNRS, at varying altitudes from 50 m to 2000 m a.g.l.

Two different air masses are identified by the back-trajectories: (1) one air mass skirts the Mediterranean coast from the east-south-east (Figure 7a). This air mass corresponds to layers *A*, *B* and *C* displayed by the radial velocity cross sections (Figure 6). The large-scale outputs indicate that the air mass originates from the south over the Mediterranean sea. Blowing along the western coast of Italy, it is diverted westward in the Gulf of Genoa, before reaching Marseille. One can note that model 2 outputs are insufficiently resolved in space to accurately differentiate the trajectories that have their end in layers *A*, *B* and *C*; (2) a second air mass is advected by a strong synoptic flow, which turns from south to south-west with altitude and is observed on the large-scale outputs over the Mediterranean Sea from Spain to Italy (Figure 7b). The air mass corresponds to layer *D*. The height of these layers evolves in the course of the day. The south-west flow is simulated above 800–1100 m a.g.l. at 1100 UTC (1100 m in the north of Marseille, and 800 m in the city centre), and above about 1500 m a.g.l. at 1400 and 1700 UTC. This is confirmed by the vertical sections of radial velocity (Figure 6b, d and f).

5.2. Shallow and deep sea breezes

According to the analysis of the horizontal wind fields of model 2, the sea breeze commences at 0900 UTC and lasts until 1900–2000 UTC on the Mediterranean coast. In the first 250 m, a shallow sea breeze (SSB) breaks through, as also observed by Bastin et al. (2004) during 25 June 2001 (see also Banta, 1995 for SSB observation on the Californian coast). The SSB is driven by the local coastal temperature gradient and thus blows perpendicular to the coastline. Indeed, in Figure 8a, the wind tries to turn towards the maximum temperature gradient direction. Because of the shape of the Marseille coastline (the city faces the sea both to the east and to the south), the SSB blows from the south-south-east south of Marseille, and from the west over the northern districts. A deep sea breeze (DSB) flows at higher levels from the east-south-east (Figure 8b) combined with the synoptic flow from the east-south-east at 1000 m a.s.l. (Figure 8c) and veering to the south-west with altitude (Figure 8d). The DSB orientation is spatially more homogeneous because it is forced by the

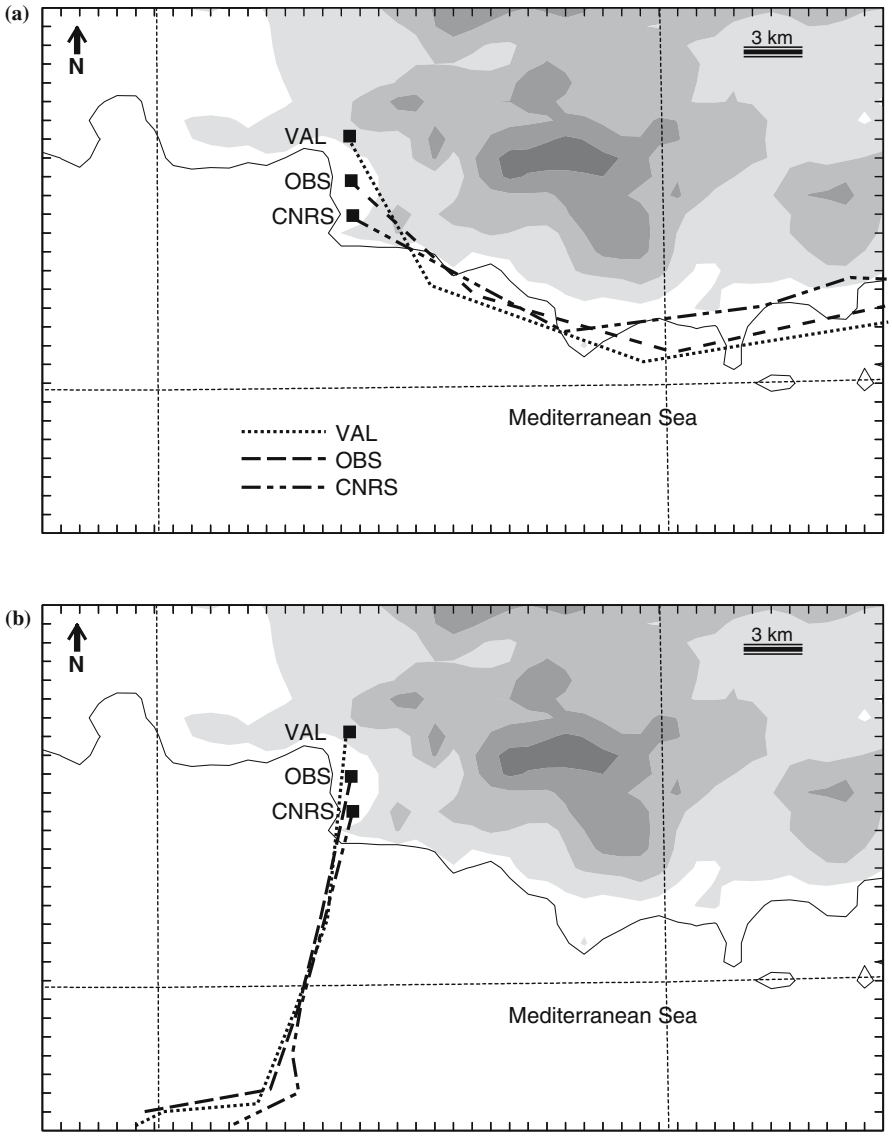

Figure 7. Back-trajectories plotted from the model 2 outputs for VAL, OBS and CNRS at (a) 50 m and (b) 900 m above the canopy. The timestep is 1 h.

regional temperature contrast between land and the Mediterranean Sea. Nevertheless, the temperature gradient oriented in the west–east direction in the northern part of the area in Figure 8b induces the rotation of the wind that veers to south-west north of Marseille, while it is southerly in the Rhône valley. Because the DSB combines with the east-south-easterly

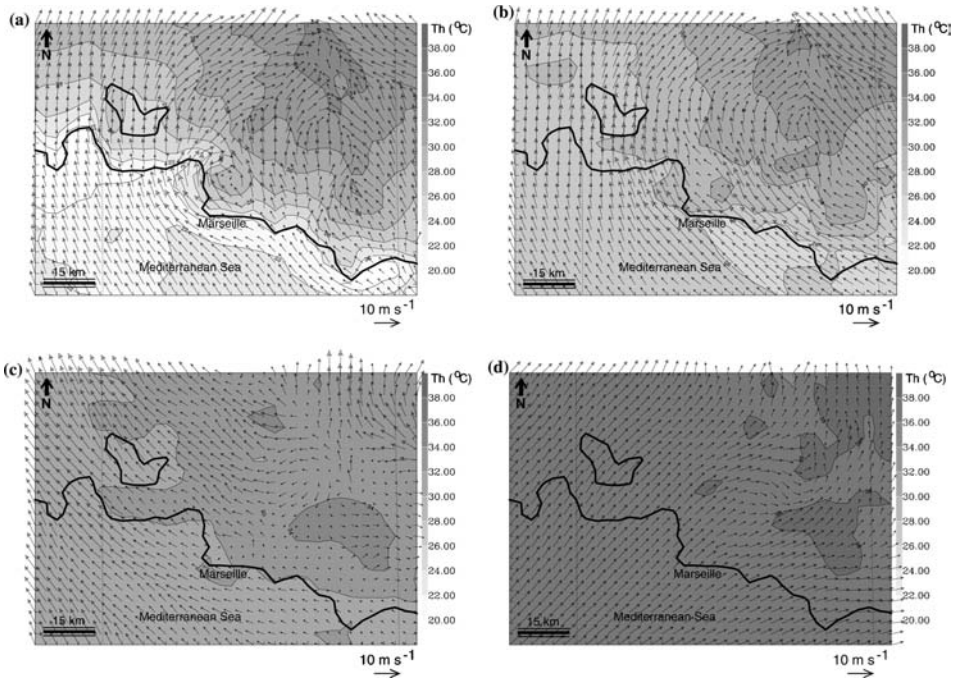

Figure 8. Horizontal wind field (arrows) superimposed to the potential temperature field, both simulated with model 2 at (a) 50 m, (b) 400 m, (c) 1000 m and (d) 2000 m above the canopy at 1400 UTC.

synoptic flow, the wind accelerates onshore (Figure 8c). Note that the disorganization of the wind in the eastern part of Figure 8c is induced by the Massif des Maures, located upstream of this area, that disturbs the easterly flow.

6. Analysis of the Local-Scale Vertical Structure

This section focuses on model 4 outputs with 250-m horizontal resolution. At the city scale, both land-use cover and topographic forcing data are defined with a higher resolution than in model 2 (see Section 3). In this case, the atmospheric circulation is complex because of the local geography. The joint analysis of the vertical cross-sections of radial velocities (Section 4), and of the vertical profiles of potential temperature and specific humidity at VAL, OBS and CNRS stations, allows a study of the evolution of the different sea-breeze circulations as well as the structure of the ABL above Marseille. Due to the undulating local topography, the structure is spatially heterogeneous at the scale of the city.

6.1. Shallow sea breezes

Figure 9 presents the horizontal wind fields at 1100 UTC (upper row) and 1400 UTC (lower row). Near the surface (panels (a) and (c)), the east-south-easterly flow is along the coast and enters the city from the south. The Puget massif (south-east of Marseille) and the Marseilleveyre massif (south-west of Marseille) affect its trajectory. Indeed, the flow is partly channelled between the two massifs, and is partly reinforced by the local sea/land temperature gradient forcing the SSB. The SSB blows from the south when it penetrates inland. However, the southerly SSB does not reach the north of the city. The horizontal wind field shows that the flow is diverted over the Mediterranean Sea by Marseilleveyre. A wake is created downstream from the Marseillveyre massif (region of stagnant air), which redirects the flow in the direction of the northern districts (Figure 9a, c). As on the southern coast, this effect initiated by the local topography is favoured and amplified by the temperature contrast on the western coast, which induces a westerly SSB. Coming from the sea to the west, the flow turns to the west-north-west at OBS and to the west-south-west at VAL. As a consequence, the southerly and westerly SSBs converge. The convergence front evolves to the advantage of the southerly SSB, which rapidly affects the city core of Marseille. The southerly SSB front progresses throughout the afternoon: it is located 9.5 km from the southern shore at 1100 UTC (Figure 9a), it reaches OBS after 1200 UTC (Figure 9c) and passes beyond OBS after 1500 UTC (not shown). This is also consistent with the surface wind data recorded at VAL, OBS and CNRS.

Figure 10 displays the comparison between the modelled (solid lines) and observed (dashed line) wind speed and direction at VAL, OBS and CNRS. At CNRS, the southerly SSB starts at 0800 UTC and persists all day long (Figure 10c). It is simulated only after 0930 UTC in the model. The modelled horizontal wind fields at 0800 and 0900 UTC (not shown) indicate that the southerly SSB has already started on the southern coast but does not reach CNRS yet. At VAL, the progressive onset of the westerly SSB is well reproduced by the model, as well as its rapid weakening after 1600 UTC (Figure 10a). The orientation is slightly shifted since the SSB blows from the west in the simulation while it blows from the west-south-west in the measurements. The situation is more complex at OBS: the station, located in the city centre, is initially under the influence of the westerly SSB, until the southerly SSB reaches OBS at 1300 UTC (Figure 10b). The modelled westerly SSB is in good agreement with the observations and the arrival of the convergence front at OBS is also correctly predicted. However, the transition between the westerly and southerly SSBs is not as clear as in the measurements because the front stabilizes around OBS, leading to a large spatial variability of the surface

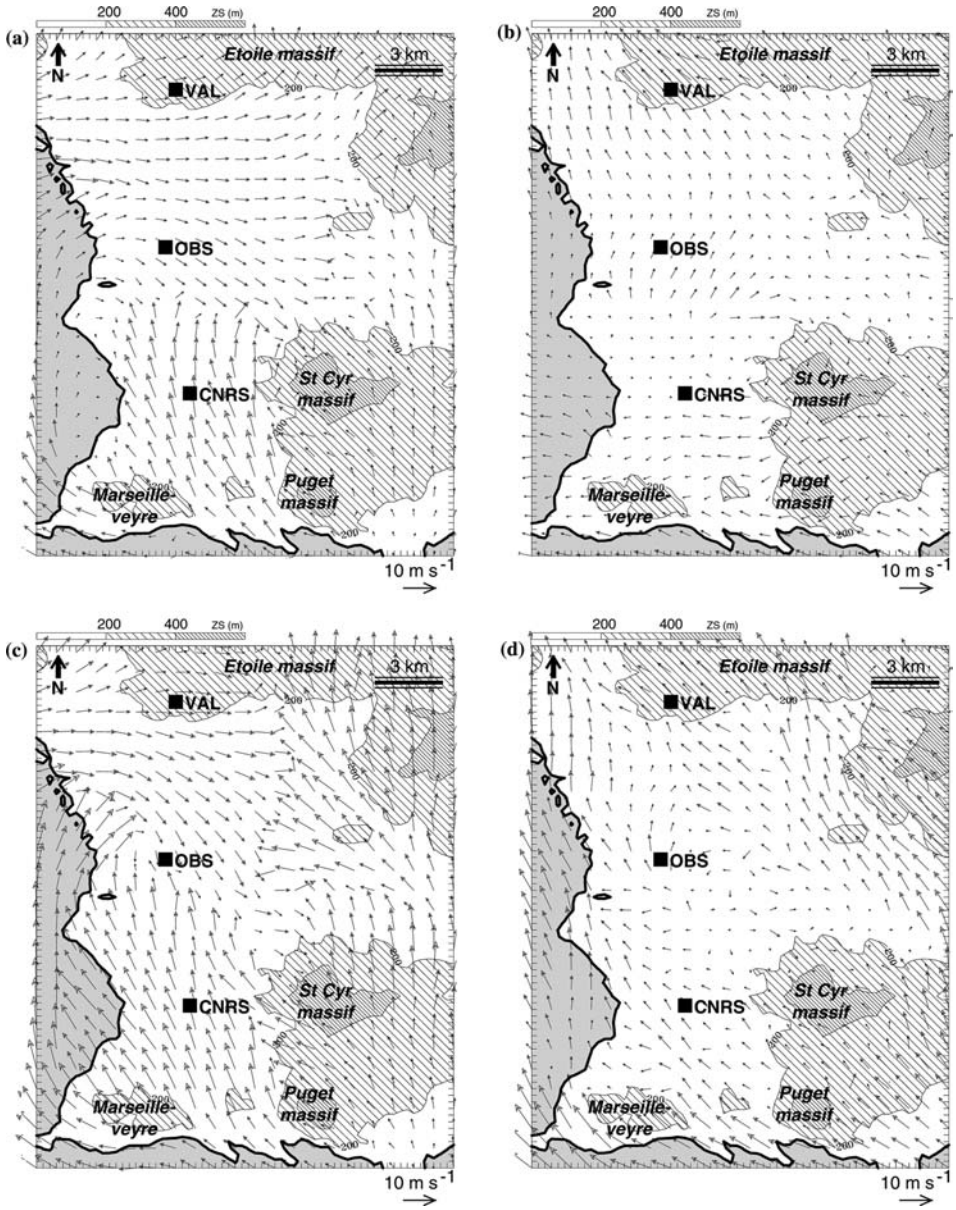

Figure 9. Horizontal wind field (arrows) simulated with model 4 at (a) 50 m and (b) 400 m above the canopy at 1100 UTC (upper row) and 1400 UTC (lower row). The shaded areas represent the local topography.

wind field around OBS between 1300 and 1600 UTC. As a consequence, even a small misprediction of the location of the SSB front can result in large local errors in the simulated wind direction. However, the impact of

these errors is very weak due to the weakness of the wind intensity at OBS (the maximum wind speed is equal to about $2\,m\,s^{-1}$). At 1600 UTC, the modelled southerly SSB front has reached OBS. Concerning the magnitude of the SSB, both observed and modelled data show that the southerly SSB is stronger than the westerly SSB: the maximum wind speed is equal to about $5\,m\,s^{-1}$ at CNRS for the southerly SSBs, and to about $3\,m\,s^{-1}$ at VAL for the westerly SSB. The stabilization of the front at the convergence zone between the westerly and southerly SSBs over OBS leads to weaker winds.

According to the vertical profiles of potential temperature and specific humidity at VAL, OBS and CNRS (Figure 11), both the southerly and westerly SSBs are associated with lower temperature and higher humidity between the surface and about 200–300 m a.s.l. than above. In detail, the southerly and westerly SSBs have different dynamic and thermodynamic characteristics. The intensity of the westerly SSB is maximum between 1400 and 1500 UTC. Indeed, at VAL, both temperature and humidity differences between the SSB and the layer above are maximum, that is about $3\,^{\circ}C$ and $2\,g\,kg^{-1}$, respectively (Figure 11a and d) and the radial velocities reach their maximum values (labelled layer *A* in Figure 6d). In comparison, the southerly SSB is less marked in the afternoon in terms of temperature and humidity contrast with the upper levels, but is associated with stronger winds. As shown previously, the southerly SSB is affected by Marseilleveyre and Puget massifs: on the one hand, the flow is channelled and accelerated between the massifs (see the wind field in Figure 9a and c); on the other hand, the flow warms up and dries over the massifs, which reduces the thermodynamic effect of the breeze inland in comparison to the westerly SSB (Figure 11c and f). The vertical extents of the westerly and southerly SSBs are also different. The westerly SSB is about 150–180 m deep (see Figure 6b, d and f), whereas the southerly SSB is about 250 m deep at 1100 UTC (Figure 11c and f). The vertical profiles indicate that the SSB keeps more or less the same extent all day long even though, in the afternoon, the southerly SSB depth is more difficult to estimate because the southerly SSB combines with the larger-scale DSB. Finally, one can note a different evolution of the vertical profiles at OBS. At 1100 UTC, the structure of the atmosphere at OBS is really similar to that at VAL (Figure 11b and e), because both are under the influence of the same flows. This was also displayed in Figure 6b by the radial velocity cross-sections. The arrival of the convergence front at 1300 UTC induces an updraft above OBS (not shown) associated with a rise of $3\,^{\circ}C$ and a reduction of almost $1.5\,g\,kg^{-1}$ in the near-surface layer.

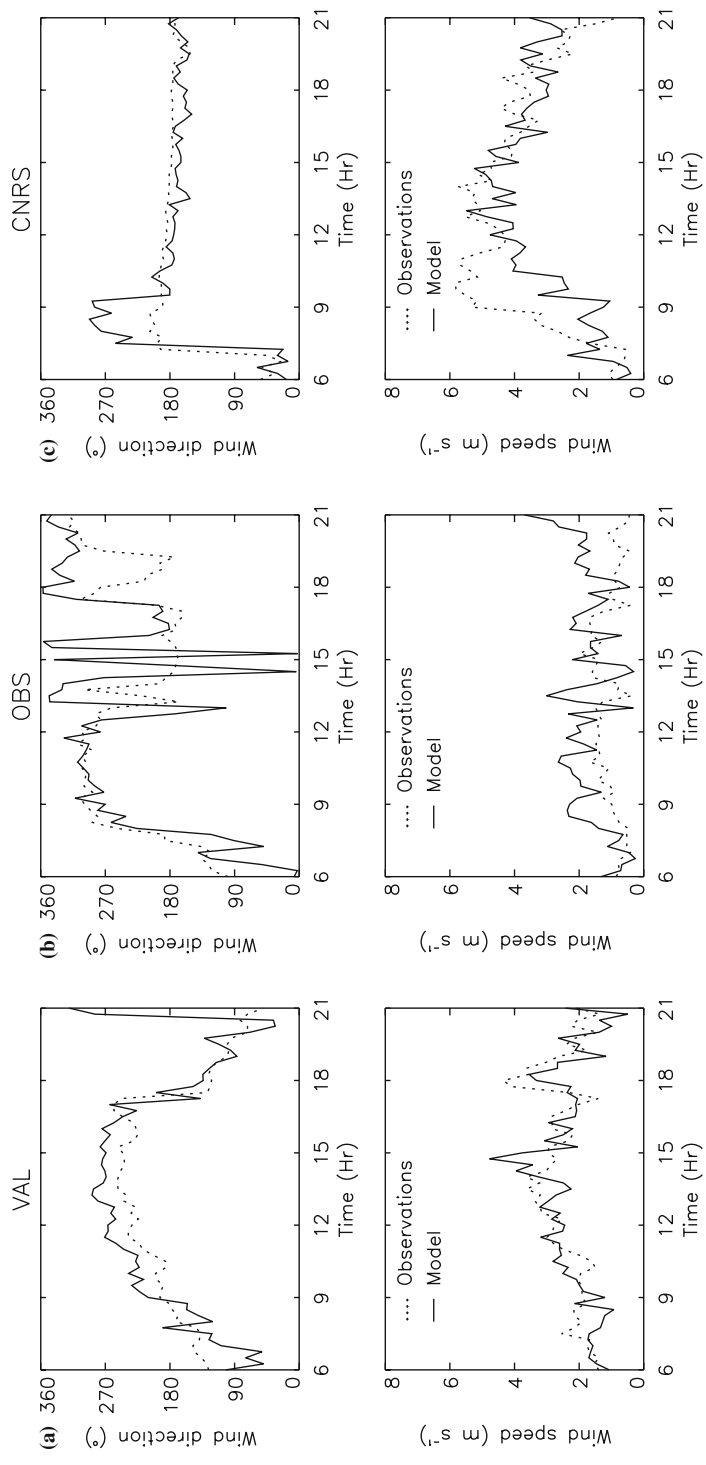

Figure 10. Comparison between modelled (solid line) and observed (dashed line) wind direction and wind speed for the (a) VAL, (b) OBS, and (c) CNRS surface stations.

6.2. Deep sea breeze

As shown in Figure 9b and d, the DSB penetrates to the south of Marseille. In contrast to the SSB, which is locally perpendicular to the coastline, the south-east direction of the DSB remains spatially homogeneous (140–150°). Compared to the SSB, the deviation of the DSB by the topography is much more attenuated but remains visible in Figure 9b and d. Indeed, two main areas of weak recirculating flow are sheltered by the different massifs: (1) the city core of Marseille in the wake trailing downstream from the Puget and Saint Cyr massifs; (2) the south-western end of the city, affected by the Puget and Marseilleveyre massifs. The comparison of the wind fields at 1100 and 1400 UTC (Figure 9b and d) shows that the sheltered area in the lee of the Puget and Marseilleveyre massifs does not evolve between 1100 and 1700 UTC, while the sheltered area in the lee of the Puget and Saint Cyr massifs is affected by the respective inland progression of the southerly and westerly SSBs: when the southerly SSB penetrates inland, the sheltered area progresses towards the city centre. In the morning, it is limited to the south of the city, whereas it reaches the OBS area after 1400 UTC. In the north of the city the DSB, which is no longer disturbed, passes beyond Marseille. Indeed, at the regional scale, the DSB is observed in all the Provence-Alpes Côte d'Azur region and penetrates about 150 km inland (Figure 5b; see also Bastin et al., 2005).

Looking at Figures 6 and 11, the DSB is deeper above the northern district of Marseille (VAL) than in the south of the city (CNRS). Indeed, the vertical profiles at VAL (Figure 11a and d) indicate that the DSB is characterized by relatively homogeneous potential temperatures and specific humidities. Its vertical extent evolves with time: the DSB is 600 m deep at 1100 UTC, 800 m deep at 1400 UTC and 600 m deep at 1700 UTC. It is also identified in Figure 6b, d and f as a layer of negative radial velocities (labelled layer *B*). The DSB presents the same vertical extension at OBS than at VAL at 1100 and 1400 UTC (Figure 11b and e). At CNRS, the layer does not exceed 450 m a.g.l. in the afternoon (Figure 11c and f). This can be caused by advection of cold air by the synoptic south-easterly flow, which stabilizes the lower troposphere near the shore and prevents the DSB development. In the northern district, the larger vertical extent of the DSB can be due to (1) the attenuated stabilizing effect that allows convection to contribute to the growth of the DSB between 1100 and 1400 UTC; (2) the sloping terrain that slows down the DSB as it starts ascending the hill (see Figure 6 between 3–4 km to the south of VAL) and thus deepens the DSB (characteristics of a supercritical flow, see Drobinski et al., 2001b). After the convergence front has passed beyond OBS, the wake downstream from the Saint Cyr massif is visible in Figure 6d and f with a core of very low radial velocities between 4 and 6 km to the south of VAL. The wake

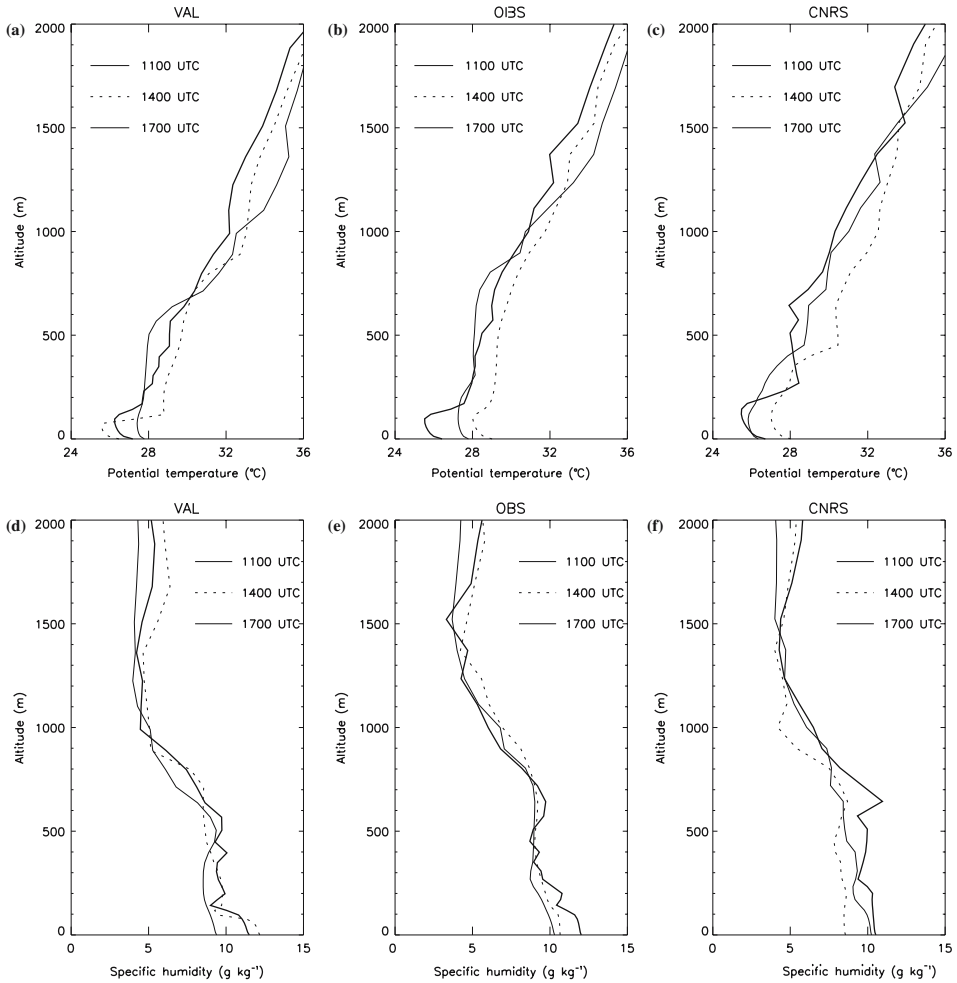

Figure 11. Vertical profiles of modelled potential temperature and specific humidity at 1100, 1400 and 1700 UTC for (a) VAL, (b) OBS, and (c) CNRS stations.

associated with hydraulic jump occurrence (Schär and Smith, 1993) results in a quasi-neutral layer between 350 and 800 m a.g.l. at OBS (Figure 11b and e) and between 450 and 700 m a.g.l. at CNRS at 1400 and 1700 UTC (Figure 11c and f).

7. Conclusion

This joint analysis of Doppler lidar measurements of radial velocity field with 300-m resolution and three-dimensional atmospheric numerical simulation

with 250-m horizontal resolution proves here to be a unique combination* to (1) validate simulated fine-scale heterogeneity of the atmospheric circulation, and (2) investigate the multi-scale forcing sources that drive the flow over the city of Marseille.

As already highlighted experimentally and numerically (with a 2-km horizontal resolution) for the 25 June 2001 sea-breeze case by Bastin et al. (2004), the analysis of the 26 June 2001 case also shows the presence of a SSB and a DSB along the Mediterranean coast. The specific study of the Marseille area reveals that the DSB flows from the south-east, perpendicular to the regional temperature gradient, whereas the SSB is composed of two branches above the city flowing perpendicular to the local temperature gradient: a southerly SSB flows perpendicular to the southern coast of the city, while a westerly SSB flows perpendicular to the western coast. Like the SSB, the DSB combined with the east-south-easterly synoptic flow below 1500 m a.g.l., is affected by the local topography when it reaches the shore near Marseille: (1) the southerly SSB and the DSB are accelerated by channelling between the Puget and Marseilleveyre massifs; (2) the southerly SSB and the DSB are deflected towards the sea by the Marseilleveyre massif; (3) two regions of weak recirculating flow (in the city core and in the south-western end of the city) are associated with wakes trailing downstream from the Saint Cyr, Puget and Marseilleveyre massifs. No urban processes are shown through this analysis, even though the modelled surface temperature fields and surface energy budgets indicate a specific signature of the city (Lemonsu et al., 2005). It seems that, under sea-breeze conditions and contrary to other cities, the impact of urban land use on the local flow dynamics over Marseille is largely inhibited. In the present case, the local flow dynamics are largely driven by the interaction between the topography and the SSB and DSB. Such fine-scale processes could not be simulated with lower resolution models, so this study reveals the interest and necessity to refine the model grid for such complex terrain.

Acknowledgements

The authors are very grateful to Dr F. Saïd (Centre de Recherches Atmosphériques, Lannemezan, France) for her assistance and Dr B. Dousset (Hawaii Institute of Geophysics and Planetology, University of Hawaii), who provided us the fields of sea surface temperature. The project UBL-ESCO-

* To our knowledge, this is the first time that such a comparison between Doppler lidar measurements and numerical model results has been conducted for a weak thermal flow, in contrast to strong valley flows (e.g. Beffrey et al., 2004; Drobinski et al., 2005b).

MPTE is funded by the CNRS programs for remote sensing from space (PNTS) and atmospheric dynamics (PATOM).

References

Banta, R. M.: 1995, 'Sea Breezes Shallow and Deep on the California Coast', *Mon. Wea. Rev.* **123**, 3614–3622.

Banta, R. M., Olivier, L. D., and Levinson, D. H.: 1993, 'Evolution of the Monterey Bay Sea-Breeze Layer as Observed by Pulsed Doppler Lidar', *J. Atmos. Sci.* **50**, 3959–3982.

Bastin, S. and Drobinski, P.: 2005, 'Temperature and Wind Velocity Oscillations Along a Gentle Slope During Sea Breeze Events', *Boundary-Layer Meteorol.* **114**, 573–594.

Bastin, S., Drobinski, P., Dabas, A. M., Delville, P., Reitebuch, O., and Werner, C.: 2005, 'Impact of the Rhône and Durance Valleys on Sea-Breeze Circulation in the Marseille Area', *Atmos. Res.* **74**, 303–328.

Bastin, S., Drobinski, P., Dabas, A. M., Delville, P., Reitebuch, O., and Werner, C.: 2004, 'Sea Breeze Case Study using a Combination of Observations and Numerial Stimulation in Complex Terrain in Southern France: Contribution to Matter Transport', *Eleventh Conference on Mountain Meteorology*, Mt Washington Valley, New Hampshire, U.S.A.

Beffrey, G., Jaubert, G., and Dabas, A. M.: 2004, 'Foehn Flow and Stable Air-Mass in the Rhine Valley: The Beginning of a MAP Event', *Quart. J. Roy. Meteorol. Soc.* **130**, 541–560.

Calhoun, R., Heap, R. B., Princevac, M., Sommer, J., Fernando, H. J. S., and Ligon, D.: 2004, 'Measurement of Winds Flowing Toward an Urban Area Using Coherent Doppler Lidar', *Fifth Conference on Urban Environment*, Vancouver, Canada.

Carroll, J. J.: 1989, 'Analysis of Airborne Doppler Lidar Measurements of the Extended California Sea Breeze', *J. Atmos. Ocean. Technol.* **6**, 820–831.

CEC: 1993, 'CORINE Land Cover, Technical Guide', *Technical Report EUR 1285 EN*, Office for the Official Publications of the European Communities, Luxembourg.

Chiba, O., Kobayashi, F., Naito, G., and Sassa, K.: 1999, 'Helicopter Observations of the Sea Breeze over a Coastal Area', *J. Appl. Meteorol.* **38**, 481–492.

Cros, B., Durand, P., Cachier, H., Drobinski, P., Frejafon, E., Kottmeier, C., Perros, P. E., Peuch, V.-H., Ponche, J. L., Robin, D., Saïd, F., Toupance, G., and Wortham, H.: 2004, 'The ESCOMPTE Program: An Overview', *Atmos. Res.* **69**, 241–279.

Darby, L. S., Banta, R. M., and Pielke, R. A.: 2002, 'Comparisons between Mesoscale Model Terrain Sensitivity Studies and Doppler Lidar Measurements of the Sea Breeze at Monterey Bay', *Mon. Wea. Rev.* **130**, 2813–2838.

Davies, F., Collier, C. G., Pearson, G. N., and Bozier, K. E.: 2004, 'Doppler Lidar Measurements of Turbulent Structure Function over an Urban Area', *J. Atmos. Ocean. Technol.* **21**, 753–761.

Deardorff, J. W.: 1974, 'Three-Dimensional Numerical Study of Turbulence in an Entraining Mixed Layer', *Boundary-Layer Meteorol.* **7**, 199–126.

Delbarre, S., Augustin, P., Freville, P., Campistron, B., Saïd, F., Bénech, B., Lohou, F., Puygrenier, V., and Fréjafon, E.: 2005, 'Ground-Based Remote Sensing Observation of the Complex Behaviour of the Marseille Boundary Layer during ESCOMPTE', *Atmos. Res.* **74**(1–4), 403–433.

Dousset, B. and Kermadi, S.: 2003, 'Satellites Observation over the Marseille-Berre Area during the UBL/CLU-ESCOMPTE Experiment', *Fifth International Conference on Urban Climate*, Łódź, Poland.

Drobinski, P., Bastin, S., Guénard, V., Caccia, J.-L., Dabas, A. M., Delville, P., Protat, A., Reitebuch, O., and Werner, C.: 2005, 'Summer Mistral at the Exit of the Rhône Valley', *Quart. J. Roy. Meteorol. Soc.* **131**, 353–375.

Drobinski, P., Brown, R. A., Flamant, P. H., and Pelon, J.: 1998, 'Evidence of Organized Large Eddies by Ground-Based Doppler Lidar, Sonic Anemometer and Sodar', *Boundary-Layer Meteorol.* **88**, 343–361.

Drobinski, P., Dabas, A. M., Haeberli, C., and Flamant, P. H.: 2001a, 'On the Small-Scale Dynamics of Flow Splitting in the Rhine Valley during a Shallow South Foehn Event', *Boundary-Layer Meteorol.* **99**, 277–296.

Drobinski, P., Dusek, J., and Flamant, C.: 2001b, 'Diagnostics of Hydraulic Jump and Gap Flow in Stratified Flows over Topography', *Boundary-Layer Meteorol.* **98**, 475–495.

Drobinski, P., Haeberli, C., Richard, E., Lothon, M., Dabas, A. M., Flamant, P. H., Furger, M., and Steinacker, R.: 2003, 'Scale Interaction Processes during the MAP IOP 12 South Foehn Event in the Rhine Valley', *Quart. J. Roy. Meteorol. Soc.* **129**, 729–753.

Estoque, M. A.: 1962, 'The Sea Breeze as a Function of the Prevailing Synoptic Situation', *J. Atmos. Sci.* **19**, 244–250.

Finkele, K., Hacker, J. M., Kraus, H., and Byron-Scott, R. A. D.: 1995, 'A Complete Sea Breeze Circulation Cell Derived from Aircraft Observations', *Boundary-Layer Meteorol.* **73**, 299–317.

Grimmond, C. S. B., Salmond, J., Oke, T. R., Offerle, B., and Lemonsu, A.: 2004, 'Flux and Turbulence Measurements at a Densely Built-Up Site in Marseille: Heat, Mass (Water, Carbon Dioxide) and Momentum', *J. Geophys. Res.* **109**, D24101, doi:10.1029/2004JD004936.

Guénard, V., Drobinski, P., Caccia, J.-L., Campistron, B., and Bénech, B.: 2005, 'Experimental Investigation of the Mesoscale Dynamics of the Mistral', *Boundary-Layer Meteorol.* **115**, 263–288.

Kambezidis, H. D., Peppes, A. A., and Melas, D.: 1995, 'An Environmental Experiment over Athens Urban Area under Sea Breeze Conditions', *Atmos. Res.* **36**, 139–156.

Lafore, J.-P., Stein, J., Asencio, N., Bougeault, P., Ducrocq, V., Duron, J., Fischer, C., Héreil, P., Mascart, P., Masson, V., Pinty, J.-P., Redelsperger, J.-L., Richard, E., and Vilà-Guerau de Arellano, J.: 1998, 'The Meso-Nh atmospheric simulation system. Part I: Adiabatic Formulation and Control Simulation', *Ann. Geophys.* **16**, 90–109.

Lemonsu, A., Grimmond, C. S. B., and Masson, V.: 2004, 'Modelisation of the Surface Energy Budget of an Old Mediterranean City Core', *J. Appl. Meteorol.* **43**, 312–327.

Lemonsu, A., Pigeon, G., Masson, V., and Moppert, C.: 2005, 'Sea-Town Interaction over Marseille: 3D Urban Boundary Layer and Thermodynamic Fields near the Surface', *Theor. Appl. Clim.*, in press.

Lemonsu, A. and Masson, V.: 2002, 'Simulation of a Summer Urban Breeze over Paris', *Boundary-Layer Meteorol.* **104**, 463–490.

Masson, V.: 2000, 'A Physically-Based Scheme for the Urban Energy Budget in Atmospheric Models', *Boundary-Layer Meteorol.* **94**, 357–397.

Mestayer, P., Durand, P., Augustin, P., Bastin, S., Bonnefond, J.-M., Bénech, B., Campistron, B., Coppalle, A., Delbarre, H., Dousset, B., Drobinski, P., Druilhet, A., Fréjafon, E., Grimmond, S., Groleau, D., Irvine, M., Kergomard, C., Kermadi, S., Lagouarde, J.-P., Lemonsu, A., Lohou, F., Long, N., Masson, V., Moppert, C., Noilhan, J., Offerle, B., Oke, T., Pigeon, G., Puygrenier, V., Roberts, S., Rosant, J.-M., Saïd, F., Salmond, J., Talbaut, M., and Voogt, J.: 2005, 'The Urban Boundary Layer Field Experiment over Marseille UBL/CLU-ESCOMPTE: Experimental Set-up and First Results', *Boundary-Layer Meteorol.* **114**, 315–365.

Noilhan, J. and Planton, S.: 1989, 'A Simple Parameterization of Land Surface Processes for Meteorological Models', *Mon. Wea. Rev.* **117**, 536–549.

Ohashi, Y. and Kida, H.: 2002, 'Effects of Mountains and Urban Areas on Daytime Local-Circulations in the Osaka and Kyoto Region', *J. Meteorol. Soc. Japan* **80**, 539–560.

Physick, W. L. and Byron-Scott, R. A. D.: 1977, 'Observations of the Sea Breeze in the Vicinity of a Gulf', *Weather* **32**, 373–381.

Pooler, F.: 1963, 'Airflow over the City in Terrain of Moderate Relief', *J. Appl. Meteorol.* **2**, 446–455.

Schär, C. and Smith, R. B.: 1993, 'Shallow-Water Flow Past Isolated Topography. Part I: Vorticity Production and Wake Formation', *J. Atmos. Sci.* **50**, 1373–1400.

Vukovich, F. M., King, W. J., Dunn, J. W., and Worth, J. J. B.: 1979, 'Observations and Simulations of the Diurnal Variation of the Urban Heat Island Circulation and Associated Variations of the Ozone Distribution: A Case Study', *J. Appl. Meteorol.* **18**, 836–854.

Yoshikado, H. and Kondo, H.: 1989, 'Inland Penetration of the Sea Breeze in the Suburban Area of Tokyo', *Boundary-Layer Meteorol.* **48**, 389–407.

Yoshikado, H.: 1990, 'Vertical Structure of the Sea Breeze Penetrating through a Large Urban Complex', *J. Appl. Meteorol.* **29**, 878–891.